THE *HUBBLE SPACE TELESCOPE* EXTRAGALACTIC DISTANCE SCALE KEY PROJECT II: [1] PHOTOMETRY OF WFC IMAGES OF M81 [2]

Shaun M. Hughes, Barry F. Madore[3] and Jeremy R. Mould
California Institute of Technology, MS 105-24
Pasadena, CA 91125
I: smh@phobos.caltech.edu, jrm@deimos.caltech.edu, barry@ipac.caltech.edu

Laura Ferrarese and Holland C. Ford
Space Telescope Science Institute
Homewood Campus
Baltimore, MD 21218
I: ferrarese@scivax.stsci.edu, ford@scivax.stsci.edu

Wendy L. Freedman[3], Robert Hill and Myung Gyoon Lee
Carnegie Observatories
813 Santa Barbara St
Pasadena, CA 91101
I: wendy@ociw.edu, bhill@ociw.edu, mglee@ociw.edu

John A. Graham
Department of Terrestrial Magnetism
Carnegie Institution of Washington
5241 Broad Branch Rd. N.W.
Washington, DC 20015
I: graham@jag.ciw.edu

John G. Hoessel
Department of Astronomy
University of Wisconsin
475 N. Charter St
Madison, WI 53706
hoessel@uwfpc.span

[1] **Based on observations with the NASA/ESA *Hubble Space Telescope*, obtained at the Space Telescope Science Institute, which is operated by the Association of Universities for Research in Astronomy, Inc., under NASA contract** NAS5-26555.

[2] **Based in part on observations made at Palomar *Observatory*, which is owned and operated by the California Institute** of Technology **(Cal tech)**. The Palomar 1.5m **telescope is jointly owned by Caltech and the Carnegie Observatories.**

[3] Visiting **astronomer at the Canada- Prance-} Iawaii Telescope, which is operated by NRC Canada, CNRS France, and** the University **of** Hawaii

John Huchra
Harvard College
Center for Astrophysics
60 Garden St
Cambridge, MA 02138
huchra@cfa3.span

Garth D. Illingworth
Lick Observatory
University of California
Santa Cruz, CA 95064
I: gdi@helios.ucsc.edu

Robert C. Kennicutt and Anne Turner
Steward Observatory
University of Arizona
Tucson, AZ 85721
I: robk@as.arizona.edu, aturner@as.arizona.edu

Peter B. Stetson
National Research Council
Dominion Astrophysical Observatory
5071 W. Saanich Rd
Victoria, BC V8X 4M6
I: stetson@dao.nrc.ca

Subject headings: calibration: photometry ---- galaxies: individual (M81)

6 August 1993

Received .....

Address for proofs:
Shaun M. Hughes
Robinson laboratory, 105-24
California Institute of 'J'ethnology
Pasadena, CA 91125

Abstract

The Extragalactic Distance Scale (HO) Key Project for Hubble Space Telescope (*HST*) aims to employ the Cepheid period-luminosity (P-L) relation to measure galaxy distances out as far as the Virgo cluster. The vital steps in this program are (1) to obtain reliable photometry of stellar images from the Wide Field Camera (WFC) exposures of selected galaxies (and from WFPC 2 after the *HST* servicing mission), and (2) to calibrate this photometry to obtain reliable distances to these galaxies from the Cepheid *P-L* relation. We have used the ALLFRAME program (based on DAOPHOT-II) to determine 28 instrumental magnitudes — 22 of F555W ($\sim V$) and 6 of F785LP ($\sim I$) – of all stars brighter than $V \sim 25.5$ in each of two 2.56x2.56 arcmin WFC fields of M81. The reductions use a varying point-spread function to account for the field effects in the WFC optics, and yield instrumental magnitudes with single epoch precision ranging from 0.09 to 0.24 mag, at $V \sim 21.8$ to 23.8 — the magnitude range of the ~30 Cepheids that we have now identified in M81. The photometric calibration onto the Johnson V and F785LP systems was determined from independent ground-based CCD observing at the CFHT 3.6m (confirmed by the KPNO 4.0m) and from the Palomar 5.0m (using the wide-field COSMIC camera) and 1.5m telescopes. Secondary standards, taken from the COSMIC and CFHT frames, were established in each of the WFC fields in Johnson V and Cousins I, allowing a direct transformation from ALLFRAME magnitudes to calibrated V and F785LP magnitudes, giving mean $V \sim 23$ magnitudes accurate to $\sim \pm 0.1$ msg.

1. Introduction

There are now several relatively precise methods for measuring distances to distant ($\lesssim 100$ Mpc) galaxies, using secondary distance indicators (eg surface brightness fluctuations for elliptical; IR Tully-Fisher relation for spirals; planetary nebulae luminosity functions; type Ia supernovae luminosities), but there are still uncertainties as to the zero-points for each of these methods. The goal of the Extragalactic Distance Scale Key Project is to use a reliable primary distance indicator (Cepheids) to measure distances of a variety of galaxies out to the Virgo cluster, and from these distances, establish the zero- points for the secondary dist ante indicators (Mould et al 1993). These calibrated secondary distance indicators should then be capable of measuring Hubble's expansion parameter (Ho) to an accuracy of *10%*.

Although *HST*'s aberrated optics rule out the use of the WFC of WF/PC 1 for most of the target galaxies of the Extragalactic Distance Scale (H_0) key project — postponing most observations until after WFPC 2 is installed — M81 is sufficiently close that 15% of a typical Cepheid's luminosity (which is the fraction of a star's apparent luminosity that is sampled in the core of WFC's point-spread function) is bright enough to be identified in the two moderately crowded fields that were selected. Thus an early start was made in developing and testing appropriate photometry routines that could both cope with undersampled images with high cosmic-ray counts, and take advantage of multi-epoch images of the same field, that are necessary for identifying Cepheids and determining their periods. Two fields in M81 were chosen. The first included V30 (one of only two Cepheids known from ground-based observations - see Freedman & Madore 1988), and the other was chosen to sample the major axis of M81, ~5.5 arcmin from the nucleus. *V* and *I* *P-L* relations for the M81 WFC data and a distance modulus have been presented in Freedman et al. (1993). Here we present a detailed discussion of the calibration of these data, color-magnitude diagrams and luminosity functions.

As a compromise between Cepheid pulsation amplitude (which decreases with increasing wavelength) and mean magnitude accuracy (which improves with increasing wavelength, due to the reduced amplitude, as well as reduced extinction uncertainties), 22 of the WFC exposures of each field were made using the F555W filter, which covers a similar bandpass to the Johnson *V* filter. An additional 6 exposures were made using the F785LP filter (similar to Kron-Cousins *I*) in order to establish a mean reddening for the Cepheids (eg Freedman *et* al. 1992).

After the Cepheids have been found, the important part is to calibrate their magnitudes, as it is from these that the P-L relation is used to measure their distance. However, calibration of WFC photometry onto a standard system is by no means straightforward. The spherical aberration causes variations in the shape of the point-spread function (PSF) across each chip, which includes changes in the ratio of the PSF's core to halo luminosity. More importantly, the WFC flatfields are obtained from earth-streaked exposures, none of which are entirely flat (deviations from flatness may be as large as 20% - Phillips 1993), and there exists a time variation of detector sensitivity due to contamination of up to 0.15 mag in F555W (Ritchie & MacKenty 1993; Labhardt et al 1993). The problems are thoroughly discussed in the WF/PC Final Orbital/ Science Verification Report (Faber and Westphal 1992, the '11) '1' Report'). In order to account for all these effects, we chose to establish a set of

secondary standards in each of the WI?C M81 fields, obtained from ground-based photometry of the brighter stars.

2. Ground-based Photometry

A variety of telescopes were used to obtain photometry of the M81 fields and to verify our calibrations. *BVRI* observations from the Canada-France-Hawaii Telescope (CFHT) were obtained on 1988 January 19-21 of the then only known Cepheids V30 and V2 (Madore, Freedman & Lee 1993; Freedman & Madore 1988). Lower S/N data were also obtained at the Palomar 1.5m by M. G. Lee on 1992 June 26, which confirmed the CFHT calibration at a level of 0.03 mag at *V* and 0.01 mag at *I*. Further confirmation that the CFHT night was photometric and the calibration reliable is inferred from a comparison of photometry of NGC 2403 obtained on the CFHT on the same night as the M81 frame, and on the Kitt Peak National Observatory (KPNO) 4m on 1984 March 23 by Madore and Freedman, which agree to better than $\pm$ 0.02 mag for *BVR* and *I* (Freedman, Lee & Madore 1993).

Unfortunately, the CFHT photometry has a small field of view, and only covers a little more than half the M81 V30 field, and none of the major axis field. This was remedied by observations with the Palomar 5m on the nights of 1992 June 8 and 9, using the COSMIC camera at the prime focus, with Johnson *V* and Gunn *i* filters. COSMIC was built by the Carnegie Observatories, and has a 2048x2048 Tektronix CCD with a gain of 3.8 electrons/ADU, a readout noise of 6.6 ADU, and a field of view of 9.5 arcmin squared. Table 1 lists the object and standard fields observed, plus their exposure time (seconds), universal time and airmass. All frames were bias-subtracted and divided by flat fields. For the *V* exposures, the flat fields for each night were obtained from a median of several twilight sky exposures. However, for the *i* flat field of June 8, only one twilight sky was obtained. This was used to characterize the general field variations due to vignetting, etc, by fitting a spline surface (with 3 knots). The pixel-to-pixel variations were obtained from a median of several dome exposures. To remove unwanted variations due to non-uniform dome illumination, this was divided by a spline-fitted surface. The real surface variations in the *i* flat were then restored by multiplying this by the surface fitted to the twilight flat.

Photometry of the stellar images was determined from both synthetic aperture and PSF-fitting photometry, using DAOPHOT (Stetson 1987) and AI, I, STAR (a second-generation profile-fitting algorithm which simultaneously fits overlapping profiles to all stars contained within a CCD image).

Samples of the stellar PSF were obtained from ~20-50 visually isolated stars in each exposure (to allow for seeing variations between exposures). The aperture magnitudes as a function of aperture radius were inspected for each PSF star, and those that were markedly discrepant were discarded (as they were probable merged stars, HII regions, clusters or background galaxies). Tots] magnitudes for the PSF stars were determined by fitting growth curves to the aperture photometry, where aperture radii ranged from 2 to 20 pixels, using DAOGROW (Stetson 1990). The mean differences between these total magnitudes and the AI, LSTAR(PSF) magnitudes were used to correct the ALLSTAR photometry of all stellar images to total magnitudes.

These ALLSTAR-derived total magnitudes (v_{tot} and i_{tot}) were then corrected for atmospheric extinction (a function of airmass X) and varying exposure times (τ), as:

v' = $v_{tot} - k_v X + 2.5\log\tau_v$, where k_v = 0.256

$i' = i_{tot} - k_i X + 2.5\log\tau_i$, where k_i = 0.155

Due to the eruption of Mt Pinatubo on 1991 June 15, the atmospheric extinction was higher than usual. The extinction corrections *(k)* were determined by M.G. Lee from Palomar 1.5 m photometry during 1992 June 21 to 25. (The standard Palomar values are k_v = 0.143 and k_i = 0.056.)

Transformations to the standard Johnson *V* and Kron-Cousins *I* systems were made by least-squares fits to $v' - V$ and $V - I$ *vs* $v' - i'$, using the published *V* and *I* magnitudes in the Table 1 references (see Figure 1). Observations at Palomar with the Gunn *i* filter are routinely transformed to the Cousins system, and there is no color term (Tinney 1993). The night of June 8, although appearing clear, was perhaps smoggy at the start, as the v' mags were observed to decrease by ~0.1 mag between each of the PG1323, M92 and SA110 exposures. The v' – *V* transform was therefore derived from PG1323, as it was taken immediately after the M81 fields. However, having no *i* exposure for PG 1323, the $V - I$ transform was derived from M92 and SA1 10. The night of June 9 seemed to be photometric, but the transforms were derived from only the PG1323, PG1633 and G67-23 fields, as the M92 magnitudes were discrepant.

The adopted transformations are:

June 8 v' – V = –0.163(.001) – 0.026(.003)* [v' – i'], σ = 0.003, N = 3
$V - I$ = 0.390(.003)+ 1.009(.002)* [v' – i'], σ = ().()56, N = 8

June 9 v' – V = –0.367(.002) – 0.035(.003)* [v' – i'], σ = 0.011, N = 11
$V - I$ = 0.394(.003) + 0.998(.002)* [V' – i']> σ = 0.060, N = 11

The change in sensitivity between the two nights, as indicated by the $\sim$ 0.2 mag difference in v' – V zero points, is due to a different normalization used in the flat fields (corresponding to –0.07 mag from June 8 to June 9) and a decrease in sensitivity on the first night of 0..12 mag, due presumably to increased extinction (as determined from PG1323 – a standard field taken on both nights at an almost identical airmass). The results of these transformations were confirmed by the CFHT photometry, which covered a portion of the V30 field. A comparison of the common secondary standards between the COSMIC and CFHT photometry (Table 4) yielded agreement at a level of +0.05 $\pm$ 0.03 in V and +0.06 $\pm$ 0.03 mag in V –]. As well, there were large areas of overlap between many of the exposures. The CFHT field overlapped with the Palomar 5m V30 field of June 8, which itself overlapped with both Palomar 5m major axis fields (which were rotated 90 degrees from each other between June 8 and 9). Figure 2 shows the scatter in V between all stars with ALLSTAR uncertainties < 0.1 mag in the CFHT/V30 (Palomar 5m) overlap. The discrepancies between the $V \leq 21$ magnitudes (and ALLSTAR, uncertainties <0.1 mag) of the stars in all the 'overlap' regions, given in Table 2, shows that all the ground-based photometry sets agree in the mean to better than 0.04 msg.

3. *HST* WFC Photometry

The 22 F555W and 6 F785LP exposures of the V30 field were acquired on the dates and for the exposure times (in seconds) given in Table 3, which also lists the rootnames that identifies each exposure in the *HST* archive. The exposure times were identical for the major axis field exposures, which were observed immediately prior to each of the V30 exposures. The *HST* frames were passed through STScI's Routine Science Data Processing calibration pipeline (Lauer 1989), which makes a correction for the analogue to digital conversion, subtracts bias and dark frames, and divides by flat-fields. For the F555W frames, a better earth-streak derived flat field was obtained in early 1992, and so all frames acquired prior to this were reprocessed through the pipeline. Although contamination effects (called measles) have been reported in shorter wavelength images, no evidence was found for this effect in any of our F555W and F785LP frames.

Although the aberrated optics of *HST* results in 85% of each star's light being spread over a 3 arcsec halo, the crowding in the two M81 fields is too severe and the background 'sky' (from the faint unresolved stars in M81) is too bright for the halo light to be measured with any acceptable degree of precision. Hence we are restricted to photometry based on fitting the central cores. However, these cores are undersampled, and so most photometry programs that fit conventional Gaussian-like PSFS are inappropriate. The two better known programs that have been suitably modified to handle WFC PSFs are: DAOPHOT II (Stetson 1992), which includes the fitting of a Lorentz function as one of its options; and DoPHOT 2.0 (based on Mateo & Schechter's 1989 DoPHOT program), but with its pseudo-Gaussian routine replaced by a *HST* PSF-like routine written by Saha (STScI). Although both programs give similar results at the faint magnitude level of the Cepheids in M81, DAOPHOT II gives better results at brighter magnitudes (Hughes 1992). However, we chose to use DAOPHOT 11 principally because Stetson (1993, in preparation) has written a modified version of ALLSTAR, called ALLFRAME, which takes advantage of the multi-epoch nature of the M81 photometry (Freedman et al 1993). Briefly, ALLFRAME is a third generation algorithm which simultaneously fits profiles to all stars contained within an ensemble of CCD images for a given field. It takes as input a list of objects and initial coordinate transformations from each epoch to the others, plus epoch to epoch magnitude offsets (due to exposure time and sensitivity differences between epochs), and a PSF model (one for each chip/filter) with residuals which vary quadratically as a function of chip coordinates. A succession of PSF fits are made to all the objects on the list in each of the epoch frames. While it does so, ALLFRAME updates the coordinate transformations, and down-weights any pixels that deviate from the mean, thereby minimizing the effects of bad pixels and cosmic rays (Stetson 1987).

One of the major problems with most WFC images is the large number of cosmic ray events. For the exposure times used (900 or 1200 seconds in l?555W, and 1800 seconds in F785LP), a large fraction (????) of the stellar images are affected by cosmic rays. To provide a robust list of stellar objects for ALLFRAME, free of cosmic ray events, median images were created of each chip in each field, in each of the F555W and F785LP filters. The precise area covered by each exposure at each epoch is offset from every other by slight (0.3 pixels in the major axis field and 8 pixels in the F555W V30 field) and sometimes not so slight (up to 100 pixels in each coordinate in the F785LP V30 field) amounts, which were determined by identifying several isolated bright stars on each chip, and matching these .

in each of the epoch frames, to create translation and rotation transformations between each epoch (which were later used by ALLFRAME). These transformations were then used to shift each frame, before creating a median image. The median image was used only to generate the list of positions of real objects for AI, LFRAME. The ALLFRAME photometry derived from PSF fits at each of these positions was obtained from each of the single epoch frames.

For the major axis field, the PSFS used in DAOPHOT and AI, LFRAME (one for each filter) were determined from combined median images of chips 1 and 2, as this yielded enough isolated stars to derive a PSF which allowed for quadratic spatial variations in the profile (Stetson 1991, 1992). For the V30 field, the PSFS were modelled on a grid of artificial stars produced by TinyTim v2.1 (kindly provided by J. Krist, STScI) for each of the four chips, and each of the two filters. Tiny Tim was also used to search for variations in the PSF from epoch to epoch (due to telescope outgassing that causes slight changes in focus), but the differences were found to be marginal, so only one grid of stars was produced for each chip and filter, at a mean epoch.

After the ALLFRAME reductions were completed, we realised the differences in the empirical and Tiny Tim PSFs may be significant. Comparisons were made by using both PSFS in DAOPHOT/ALl,STAR reductions of a 5x5 grid of chip 2 observations of the same star (HD 151406 – FO spectral type) obtained by STScI on 1991 Nov 9 as part of their calibration database. Over the whole chip, the mean difference between the empirical and TT PSF magnitudes was only +0.03 mag, with an rms of 0,15. However, there was radial structure in the differences, and the mean magnitude difference for those stars within $\sim$300 pixels of the center of symmetry of chip 2 was +0.15, with an rms of 0.09 msg. (Unfortunately no similar grid of stars exists for the other chips, although we would expect comparable differences.) New empirical PSFS were then made for each chip, by combining the median images from the V30 and major axis fields (in order to have enough bright isolated stars in each chip). Systematic differences as a function of chip position are seen between these new and old empirical PSFS and the Tiny Tim PSFS. However, since we are calibrating the ALLFRAME mags directly against secondary standards in each of the fields, the zero-point differences were accounted for in the conversion of ALLFRAME mags ($F555W_{ALF}$ and $F785LP_{ALF}$) to standard mags (V and F785LP), and the positional differences were less than the uncertainties in the secondary standard magnitudes. For example, the rms difference between the secondary standard mags and those derived from the old and new PSFs changed from

0.07 to 0.05 (chip 1), and from 0.14 to 0.10 (chip 2) in F555W, and from 0.14 to 0.15 (chip 1), and from 0.15 to 0.12 (chip 2) in F785LP. Nevertheless, we are continuing with experiments to improve fits to the WFC PSF.

4. Calibration of WFC Photometry

Secondary standards in each of the *HST* WFC fields in M81 were established from the CFHT and Palomar photometry. These are listed in Table 4, which gives their identifying number corresponding to Figure 3c-d, their V and $V-I$ magnitudes, their ALLFRAME identifier and positions with respect to the raw (800x800 pixels) *HST* frames, and their mean ALLFRAME magnitudes. The median *HST* WFC images were used to visually inspect each potential secondary standard, to ensure they were isolated stellar images (over half the 'stellar images' identified on the COSMIC frames turned out to be HII regions or clusters on the *HST* frames).

For the 65 secondary standards used, the $V-$ F785LP colors ranged from –0.22 to 2.36 mag with a mean color of 0.48 mag, and the colors of the 31 Cepheids ranged from 0.60 to 1.65 with a mean of 1.05 msg. This color difference is equivalent to a difference in F555W$-$V $\sim$ 0.01 mag, and F785LP$-I \sim$ 0.14 mag (Harris et at 1991). We therefore ignored the color term in converting F555W mags to Johnson V, and accounted for the large color term between F785LP and Kron-Cousins I, by converting the secondary standards' I to F785LP, as per Harris et al (1991).

The mean differences between the ground-based secondary standard magnitudes and the A. LLFRAME WFC magnitudes are given in Table 5. The results for the V30 and major axis fields, which used different PSFS (see above), are equivalent at $\sim$0.1 mag in V. In F785LP the differences are larger, chip 1 being 0.4 msg. We experimented with various possible correction methods, including fitting a surface to the old empirical PSF and Tiny Tim PSF magnitude differences of synthetic stars generated by the new empirical PSF, and fitting surfaces to the F555W and F785LP flat field corrections (Phillips 1993), but none systematically reduced the field to field differences. Therefore we combine the two uncorrected results, to give a mean offset between the standard and ALL FRAME photometry, given in 'l'able 6. These results are comparable to what we can derive from the IDT Report (the numbers in parentheses in Table 6), wherein corrections have been applied for the WFC sensitivity at F555W on 1992 January 3 ($\sim$same date as the first of our M81 epochs, to which all the ALLFRAME magnitudes are transformed) and the differences in sensitivity between WFC chips (11) '1' Report Table 12.1 3), as

well as the aperture correction from ALLFRAME magnitudes to a radius of 40 pixels (measured to be 1.60 mag).

5. Color Magnitude Diagram

****
* *
* ANNE AND ROB 'S SECTION HERE *
* *
****

6. Conclusions

When the $V-\mathrm{F555W}_{ALF}$ corrections in Table 6 are applied to the ALLFRAME photometry, we derive the luminosity function in Figure 4, which is of all stars that appeared in all F555W frames from all chips and both fields, after removing any stars whose rms dispersion was more than 3 standard deviations from the mean, as these are likely to be either variables or to have been contaminated by cosmic ray hits. The turnover indicates we are complete down to $V \sim 25$, which represents the single-epoch magnitude limit for a $\sim$ 1000 sec WFC F555W exposure. The uncertainties in these magnitudes are shown in Figure 5, which plots the mean rms dispersion from the 22 F555W epochs about the mean magnitude in each of 50 magnitude bins. Also plotted here are the mean single-epoch uncertainties for each magnitude, as calculated by ALLFRAM E, and close agreement is seen down to $V \lesssim 25$, beyond which the ALLFRAME uncertainties and rms dispersions start to lose meaning, as they are for magnitudes clearly beyond the limit of WFC.

Using the calibration in Table 6, the mean V magnitudes of the Cepheids found in M81 ranged from 21.6 to 23.8 (and their periods ranged from 10 to 55 days), corresponding to single epoch magnitude uncertainties (Figure 5) of 0.1 to 0.3 mag, respectively. The uncertainties from the multi-epoch (22) magnitude sample should therefore be in the range 0.02 to 0.06 mag (but will depend on their position and environment, and how well their light curve is sampled). And combining all 30

Cepheid magnitudes results in an uncertainty in the zero point of a line of best fit to the *P-L* relation of 0.05 mag (Freedman et al 1993). 'l'he CMD analysis shows that all the Cepheids are located in the instability strip, and that the stellar populations in these two M81 fields have similar magnitudes and colors as those in the disk of M33.

In order to improve the photometric accuracy, work is continuing to better characterize the WFC PSF and its variation across each chip. In addition, we are planning to obtain deeper ground-based images of the two M81 fields, in order to have enough secondary standards to map any changes in the *HST* photometry due to the uncertain flat fields and varying PSF.

We are grateful to Alan Dressier and Bill Kens of the Carnegie Observatories for their time and effort in building the COSMIC camera for the Palomar 5m. Support for this work was provided by NASA through grant number 2227-87A from the Space Telescope Science Institute which is operated by the Association of Universities for Research in Astronomy Inc. under NASA Contract NAS5-26555. BFM is supported in part by the NASA/IPAC Extragalagtic Database (NED) and the Jet Propulsion Laboratory, Caltech. The ground-based calibration was supported in part by NSF grants A ST-87-13889 and A ST-91-16496 to WI, F.

References

Christian C. A., Adams M., Barnes J. V., Butcher H., Hayes D. S., Mould J. R., Siegel M. 1985 PASP 97, 363

Freedman W. L., Lee M. G., & Madore B. F. 1993, in preparation

Freedman W, 1,., & Madore B. F. 1988 ApJ 332, L63

Freedman W. L., et al. 1992 ApJ, 396, 80

Freedman W. I,., et al. 1993 ApJ, submitted

Harris H. C., Baum W. A., Hunter D. A., Kreidl 'T'. J. 1991 AJ 101, 677

Holtzman J. A., et al. 1991 AJ 369, 1,35

Hughes S. M. G. 1992 IAU Coll.136 Stellar *Photometry*, Dublin August 1992, in press

Labhardt 1,., Schwengeler I ., Tammann G. 1993 ST-ECF Newsletter # 19, Feb, p 13

Landolt A. U. 1992 AJ 104, 340

Lauer T. R. 1989 PASP, 101, 445

Madore B. F., Freedman W. I,., Lee M. G. 1993, in preparation

Mateo M., & Schechter P. 1989, in *1st ESO ST-ECF Data Analysis Workshop,* eds. P. J. Grosbol, F. Murtagh and R. H. Warmels (Garching:ESO), p69

Mould J. R., Kristian J., Da Costa G. S. 1983 ApJ 270, 471

Mould J. R., et al. 1993 BAAS, in press

Phillips D. 1993 *Lick MDS Report #3*

Ritchie C. E., & MacKenty J. W. 1993, *WF/PC Instrument Science Report 93-02,* STScI

Stetson P. B. 1987 PASP 99, 101

Stetson P. B. 1990 PASP 102, 932

Stetson P. B. 1991, in *Astronomical Data Analysis Software and Systems I,* ASP Conference Series Vol. 25, eds. D. M. Worrall, C. Biemesderfer, and J. Barnes, p. 297

Stetson P. B. 1992 in 3rd *ESO/ST-ECF Data Analysis Workshop,* ESO Conference and Workshop proceedings N0.38, eds. P. J. Grosbol and R. H. Warmels (Garching:ESO), p187

Tinney C. G. 1993, PhD thesis, California Institute of Technology, Pasadena, CA

TABLE 1

PALOMAR 5M OBSERVATIONS

Field	*V* exposures			i exposures		
	Exp	UT	Airmass	Exp	UT	Airmass
		---1992 June 8 ----				
M81 major axis	182	4:14	1.45	180	4:20	1.48
M81 V30 field	180	4:36	1.51	180	4:30	1.49
PG1323[a]	20	5:07	1.40	...	...	.
M92[b]	20	6:42	1.05	20	6:28	" 1.06
SA110[a]	3	11:55	1.54	3	11:52	1.49
		--- 1992 June 9 —				
PG1323[a]	5	3:50	1.35	5	3:56	1.35
M81 major axis	180	4:20	1.48	180	4:34	1.51
M92[b]	20	4:56	1.23	20	5:00	1.22
PG1633[a]	5	7:57	1.11	5	7:52	1.10
G67-23[c]	5	11:46	1.10	5	11:43	1.11

" Landolt 1992; [b]Christian et al. 1985; [c]Mould, Kristian, Da Costa 1983

TABLE 2

COMPARISON OF *V* 'OVERLAP' MAGS

Fields	N	AV	rms
V(v30) – V(CFHT)	2 2	0.04	0.06
V(v30) – V(maj_8)	133	0.02	0.12
V(v30) – V(maj_9)	154	–0.03	0.13
V(maj_8) – V(maj_9)	357	0.01	0.17

TABLE 3

HST WFC OBSERVATIONS OF M81

Date	MJD"	Exp	*HST* maj	& V30 rootnames
	--- F555W exposures ---			
1991 Dec 30	48620.867	900	WOTPO1O1T	WOTPOJOIT
1991 Dec 30	48620.879	900	WOTPO1O2T	WOTPOJ02T
1991 Dec 31	48621.803	1200	W0TP0201T	W0TP0K01T
1992 Jan 9	48630.759	1200	WOTP0301T	W0TP0L01T
1992 Jan 20	48641.150	1200	W0TP0401T	WOTPOMOIT
1992 Jan 21	48642.025	1200	WOTP0501T	WOTPONOIT
1992 Jan 22	48643.098	1200	WOTP0601T	WOTPOOOIT
1992 Jan 23	48644.633	1200	WOTP0701T	WOTPOPOIT
1992 Jan 25	48646.231	900	WOTP0801T	WOTPOQOIT
1992 Jan 25	48646.243	900	WOTP0802T	W0TP0Q02T
1992 Jan 28	48649.062	1200	WOTP0901T	WOTPOROIT
1992 Feb 1	48653.002	900	WOTPOAOIT	WOTPOSOIT
1992 Feb 1	48653.014	900	WOTPOA02T	WOTPOS02T
1992 Feb 6	48658.106	1200	WOTPOBOIT	WOTPOTOIT
1992 Feb 11	48663.053	900	WOTPOCOIT	WOTPOUOIT
1992 Feb 11	48663.065	900	WOTPOC02T	WOTPOU02T
1992 Dec 28	48984.101	1200	WOTPODOIT	WOTPOVOIT
1992 Dec 31	48987.380	1200	WOTPOEOIT	WOTPOWOIT
1993 Jan 5	48992.334	1200	WOTPOFOIT	WOTPOXOIT
1993 Jan 13	49000.162	1200	WOTPOGOIT	WOTPOYOIT
1993 Jan 25	49012.273	1200	WOTPOHOIT	WOTPOZOIT
1993 Feb 11	49029.241	1200	W0TP0I01T	WOTP1OO1T
	---- F785LP exposures ----			
1992 Jan 9	48630.815	1800	WOTP0302T	WOTPOL02T
1992 Jan 22	48643.153	1800	WOTP0602T	WOTPOO02T
1992 Jan 28	48649.113	1800	WOTP0902T	W0TP0R02T
1992 Feb 11	48663.120	1800	WOTPOC03T	WOTPOU03T
1992 Dec 31	48987.441	1800	W0TP0E02T	WOTPOW02T
1993 Jan 13	49000.291	1800	W0TP0G02T	WOTPOY02T

°MJD = modified Julian Date –2400000 days

TABLE 4

M81 SECONDARY STANDARDS

ID	v	v – I	F555W$_{ALF}$	(F555W–F785LP) $_{ALF}$	X (*HST*)	Y	ID$_{ALF}$
			--- V30 field -				
	Chip 1- PAL						
1	19.505 ± 0.012	1.063 ± 0.018	16.129 ± 0.028	0.643 ± 0.053	*104.8*	607.4	3569
2	19.641 ± 0.013	0.774 ± 0.021	16.352 ± 0.028	0.266 ± 0.056	*703.7*	156.0	759
3	21.705 ± 0.054	2.098 ± 0.063	18.404 ± 0.032	1.878 ± 0.076	*728.5*	758.5	4702
4	19.192 ± 0.013	1.198 ± 0.015	15.644 ± 0.037	0.394 ± 0.061	*203.4*	233.8	11183
	Chip 1- CFHT						
5	22.180 ± 0.060	0.260 ± 0.250	18.752 ± 0.040	-0.876 ± 0.102	296.1	403.5	2134
6	22.214 ± 0.060	0.613 ± 0.115	18.830 ± 0.032	-0.476 ± 0.083	294.6	425.7	2278
7	22.309 ± 0.103	0.222 ± 0.141	18,897 ± 0.034	-1.084 ± 0.095	310.8	203.7	1020
8	22.643 ± 0.068	0.430 ± 0.305	19.151 ± 0.038	-1.645 ± 0.169	252.0	322.8	1698
	Chip 2- PAL						
9	16.596 ± 0.011	0.856 ± 0.059	13.302 ± 0.145	-0.036 ± 0.389	493.6	300.7	1719
10	18.200 ± 0.005	1.000 ± 0.012	14.400 ± 0.051	0.167 ± 0.110	161.7	717.6	5213
11	20.139 ± 0.014	0.944 ± 0.022	16.633 ± 0.031	0.247 ± 0.059	733.0	678.5	1965
12	22.103 ± 0.089	0.454 ± 0.159	18.573 ± 0.035	-0.855 ± 0.102	331.6	652.9	4563
	Chip 2- CFHT						
13	21.968 ± 0.234	0.385 ± 0.271	18.237 ± 0.080	-0.573 ± 0.170	*58.4*	191.8	1010
14	22.318 ± 0.119	0.233 ± 0.253	18.896 ± 0.038	-0.878 ± 0.119	*252.9*	390.3	2338
15	22.881 ± 0.019	0.749 ± 0.045	19.220 ± 0.041	-0.090 ± 0.099	*137.2*	210.2	433
16	22.696 ± 0.132	0.442 ± 0.182	19.080 ± 0.080	0.370 ± 0.170	*271.6*	256.6	1417
17	22.050 ± 0.045	0.094 ± 0.100	18.350 ± 0.034	-0.687 ± 0.091	*81.4*	519.9	3359
18	22.042 ± 0.114	0.001 ± 0.140	18.175 ± 0.080	-0.908 ± 0.170	*36.7*	626.7	1750
19	22.872 ± 0.084	0.376 ± 0.147	19.222 ± 0.044	-0.969 ± 0.134	*203.2*	439.6	2721
	Chip 3- PAL						
20	17.316 ± 0.005	0.979 ± 0.017	13.471 ± 0.061	0.084 ± 0.091	703.7	*283.3*	1
21	21.894 ± 0.069	2.047 ± 0.073	18.136 ± 0.029	1.467 ± 0.058	558.4	*333.8*	55
22	20.303 ± 0.021	1.048 ± 0.030	16.587 ± 0.026	0.310 ± 0.050	468.2	*191.2*	6
23	20.689 ± 0.024	0.258 ± 0.053	17.001 ± 0.027	-0.634 ± 0.063	477.2	*156.3*	12
24	21.514 ± 0.065	0.306 ± 0.110	17.962 ± 0.027	-0.665 ± 0.059	352.0	*119.7*	46
25	21.'316 ± 0.072	0.103 ± 0.172	18.228 ± 0.029	-0.689 ± 0.083	416.1	*358.2*	68
26	22.068 ± 0.072	0.696 ± 0.118	18.490 ± 0.035	-0.340 ± 0.080	343.2	*542.5*	71
	Chip 3- CFHT						
22	20.250 ± 0.058	0.994 ± 0.054	6.587 ± 0.026	0.310 ± 0.050	468.2	191.2	6
23	20.707 ± 0.024	0.214 ± 0.042	7.001 ± 0.027	-0.634 ± 0.063	477.2	156.3	12
24	21.362 ± 0.030	0.260 ± 0.085	7.962 ± 0.027	-0.665 ± 0.059	352.0	119.7	46
25	21.998 ± 0.074	0.239 ± 0.159	8.228 ± 0.029	-0.689 ± 0.083	416.1	358.2	68
26	21.905 ± 0.044	0.563 ± 0.075	8.490 ± 0.035	-0.340 ± 0.080	343.2	542.5	71
27	20.343 ± 0.012	-0.155 ± 0.044	6.737 ± 0.028	-0.947 ± 0.061	134.5	103.5	9
28	21.268 ± 0.091	-0.011 ± 0.120	7.510 ± 0.028	-0.914 ± 0.063	156.4	99.7	30
29	21.297 ± 0.062	0.197 ± 0.299	7.704 ± 0.028	-0.571 ± 0.072	336.3	171.3	36
30	22.161 ± 0.046	0.217 ± 0.190	8.633 ± 0.031	-0.926 ± 0.074	325.5	149.5	95
31	21.686 ± 0.090	0.234 ± 0.108	7.967 ± 0.027	-0.654 ± 0.071	386.0	385.0	50
32	21.778 ± 0.034	0.014 ± 0.172	8.101 ± 0.029	-0.782 ± 0.068	366.9	203.5	53
33	22.350 ± 0.070	0.601 ± 0.087	8.674 ± 0.032	-0.606 ± 0.066	487.6	213.2	115
34	22.144 ± 0.064	0.190 ± 0.163	18.786 ± 0.033	-0.3873:0.073	502.5	245.6	121

	Chip 4- PAL						
35	17.421 ± 0.005	1.103 ± 0.021	13.881 ± 0.040	0.897 ± 0.076	611.5	499.4	8744
36	20.116 ± 0.019	0.576 ± 0.031	16.530 ± 0.027	-0.112 ± 0.051	532.0	760.1	26
37	20.173 ± 0.019	0.756 ± 0.029	16.602 ± 0.027	0.054 ± 0.051	205.8	358.6	28
38	21.625 ± 0.072	0.140 ± 0.135	18.031 ± 0.028	-0.673 ± 0.068	241.8	285.5	90
	Chip 4- CFHT						
36	20.081 ± 0.060	0.455 ± 0.060	16.530 ± 0.027	-0.112 ± 0.051	532.0	760.1	26
37	20.113 ± 0.015	0.664 ± 0.070	16.602 ± 0.027	0.054 ± 0.051	205.8	358.6	28
38	21.626 ± 0.067	0.033 ± 0.181	18.031 ± 0.028	-0.673 ± 0.068	241.8	285.5	90
39	20.966 ± 0.033	0.353 ± 0.062	17.616 ± 0.032	-0.064 ± 0.054	304.2	659.9	61
40	21.103 ± 0.058	0.161 ± 0.157	17.682 ± 0.028	-0.721 ± 0.065	163.4	79.2	50
41	20.874 ± 0.066	0.467 ± 0.098	17.906 ± 0.037	0.031 ± 0.070	242.8	85.2	54
42	21.480 ± 0.053	0.326 ± 0.091	18.011 ± 0.029	-0.533 ± 0.059	322.5	647.3	95
43	21.887 ± 0.047	0.201 ± 0.160	18.087 ± 0.031	-0.642 ± 0.070	534.8	346.4	112
44	21.473 ± 0.052	0.297 ± 0.064	18.131 ± 0.029	-0.368 ± 0.065	613.1	126.1	79
45	21.691 ± 0.003	0.205 ± 0.251	18.290 ± 0.030	-0.380 ± 0.064	241.2	369.6	115
46	22.007 ± 0.098	-0.044 ± 0.124	18.330 ± 0.028	-0.631 ± 0.056	314.9	241.8	114
47	21.954 ± 0.053	0.017 ± 0.183	18.332 ± 0.028	-0.925 ± 0.066	246.5	320.1	118
48	21.829 ± 0.070	0.175 ± 0.137	18.375 ± 0.029	-0.739 ± 0.067	461.1	665.8	127
49	22.115 ± 0.022	1.115 ± 0.073	18.408 ± 0.031	0.431 ± 0.052	542.5	226.2	140

TABLE 4 — *continued*

ID	v	$V - I$	$F555W_{ALF}$	$(F555W-F785LP)_{ALF}$	X (*HST*)	Y (*HST*)	ID_{ALF}
			— Major axis field —				
	Chip 1- PAL						
1	20.224 ± 0.023	0.759 ± 0.035	16.651 ± 0.012	0.105 ± 0.027	253.6	714.6	2271
2	20.984 ± 0.045	0.478 ± 0.069	17.503 ± 0.008	-0.544 ± 0.031	551.9	101.9	218
3	21.206 ± 0.067	-0.211 ± 0.139	17.690 ± 0.015	-0.336 ± 0.035	299.3	77.1	140
4	21.115 ± 0.058	0.129 ± 0.086	17.706 ± 0.012	-0.661 ± 0.029	315.2	551.4	1702
5	21.720 ± 0.082	0.037 ± 0.155	17.930 ± 0.010	-0.962 ± 0.042	630.1	213.0	610
6	21.606 ± 0.089	0.316 ± 0.141	18.336 ± 0.016	-0.204 ± 0.040	339.3	203.5	578
	Chip 2- PAL						
7	20.685 ± 0.032	0.164 ± 0.064	16.798 ± 0.012	-0.636 ± 0.026	136.8	582.4	3406
8	21.216 ± 0.041	0.214 ± 0.084	17.792 ± 0.014	-0.642 ± 0.033	465.4	729.2	4277
9	21.564 ± 0.072	0.212 ± 0.118	17.999 ± 0.014	-0.454 ± 0.033	261.1	480.1	2808
	Chip 3- PAL						
10	20.323 ± 0.025	-0.122 ± 0.055	16.856 ± 0.016	-0.719 ± 0.030	395.1	633.1	4546
11	21.429 ± 0.053	0.212 ± 0.091	17.675 ± 0.018	-1.347 ± 0.054	709.0	645.9	4626
	Chip 4- PAL						
12	20.855 ± 0.042	0.084 ± 0.076	17.079 ± 0.016	-1.155 ± 0.044	*773.4*	*426.3*	2860
13	20.937 ± 0.046	0.152 ± 0.082	17.203 ± 0.016	-0.651 ± 0.032	*633.4*	*209.9*	1084
14	21.166 ± 0.055	-0.092 ± 0.109	17.655 ± 0.017	-0.687 ± 0.038	*316.9*	*339.1*	2053
15	21.230 ± 0.058	1.454 ± 0.062	17.680 ± 0.016	0.815 ± 0.042	*311.6*	*714.7*	5758
16	22.019 ± 0.096	0.417 ± 0.146	18.383 ± 0.018	-0.337 ± 0.044	*564.6*	*220.2*	1150

TABLE 5

CALIBRATION OF WFC PHOTOMETRY

Chip	N	V−F555W$_{ALF}$	F785LP−F785LP$_{ALF}$
		— V30 field —	
1	8	3.40 ± 0.03	2.38 ± 0.17
2	11	3.62 ± 0.05	2.69 ± 0.12
3	15	3.64 ± 0.03	2.73 ± 0.04
4	15	3.51 ± 0.04	2.81 ± 0.05
		----- Major axis field — -	
1	6	3.51 ± 0.07	2.80 ± 0.14
2	3	3.63 ± 0.14	2.84 ± 0.15
3	2	3.61 ± 0.14	2.53 ± 0.35
4	5	3.64 ± 0.05	2.80 ± 0.07

TABLE 6

CALIBRATION OF MEAN WFC PHOTOMETRY

Chip	N	V − F555W$_{ALF}$		F785LP − F785LP$_{ALF}$	
		Ground-based	IDT Report	Ground-based	IDT Report
1	14	3.45 ± 0.04	(3.51)	2.56 ± 0.13	(2.70)
2	14	3.62 ± 0.05	(3.68)	2.72 ± 0.10	(2.73)
3	17	3.63 ± 0.03	(3.66)	2.71 ± 0.05	(2.59)
4	20	3.54 ± 0.04	(3.57)	2.80 ± 0.04	(2.59)

Figure Captions

Figure 1 v' – V and $V - I$ *vs* $v' - i'$ for the standards observed with Palomar 5m plus COSMIC camera, on 1992 June 8 (a, b) and 1992 June 9 (c, d). Circles are PG1323 standards (–086, C and B), crosses are PG1633 standards (A, B, C, D, and +099), and squares are G67-23 standards *(-23, -123, -223), as* referred to in Table 1. The dashed lines are least-squares fits to the data, and are the transformations used to convert the COSMIC photometry to standard (see text).

Figure 2 The difference in V magnitudes derived from independent exposures, for stars in the overlap region between the Palomar 5m (COSMIC) V30 field taken on 1992 June 8, and the CFHT field taken on *1988* Jan 20.

Figure 3 Full 2048x2048 COSMIC V image of the (a) V30 and (b) major axis fields in M81. The squares are the positions of the secondary standards. Corresponding mosaiced images of *HST F555W* median frames are given for the V30 (c) and major axis (d) fields, with the same standards identified as in (a) and (b), and numbered according to Table 4. 'I'he V30 field COSMIC image has north up, east to the left, with the *HST* image rotated 12 degrees north towards east, and the major axis fields are rotated by 29 degrees (COSMIC) and 41 degrees (*HST*) north towards east.

Figure 4 Calibrated V luminosity function of stars that were recovered in all 22 F555W epochs in all chips and in both M81 fields, and which had rms dispersions about their mean of less than 3 standard deviations (as these are likely to have been severely contaminated by cosmic ray hits).

Figure 5 The solid line is the mean rms dispersion about the mean of the 22 epoch magnitudes of the stare in Figure 4, for each of 50 magnitude bins. The dashed line is the mean single-epoch uncertainty given by ALLFRAME in the same magnitude bins,

Fig 1a

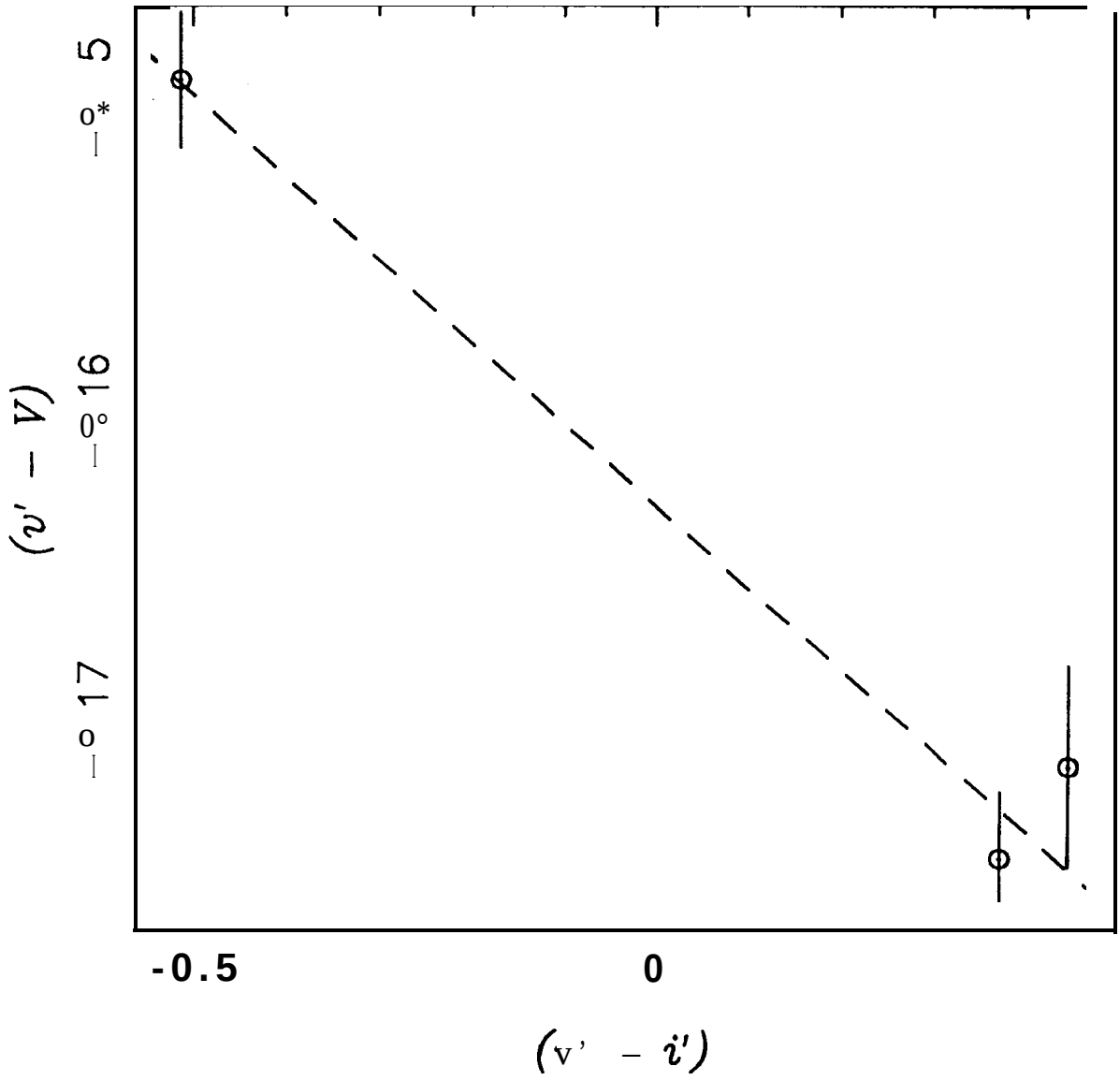

From /scr2/smh/m81/pal/stan_trans_all.f

Fig 16

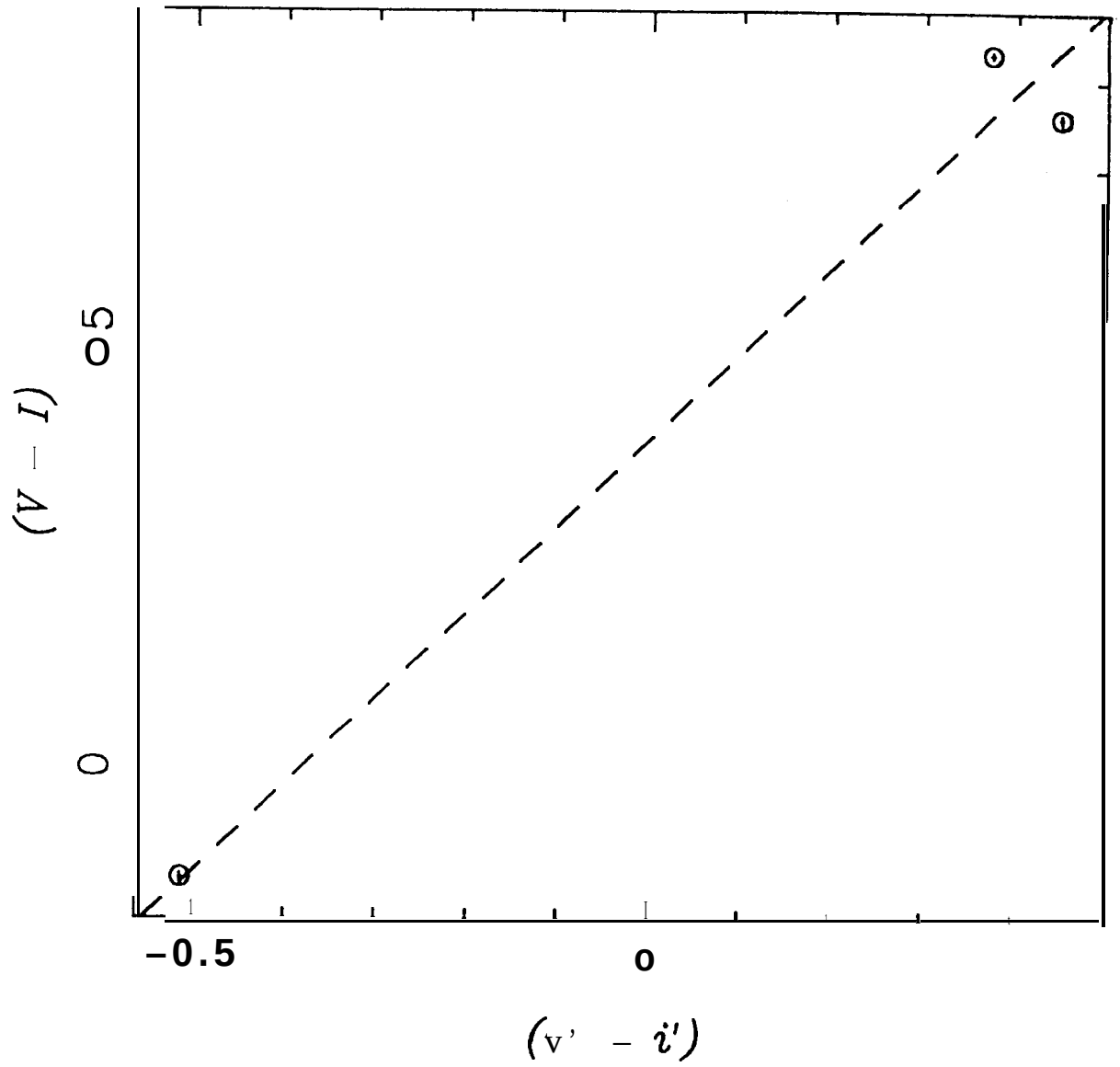

Fig 1c

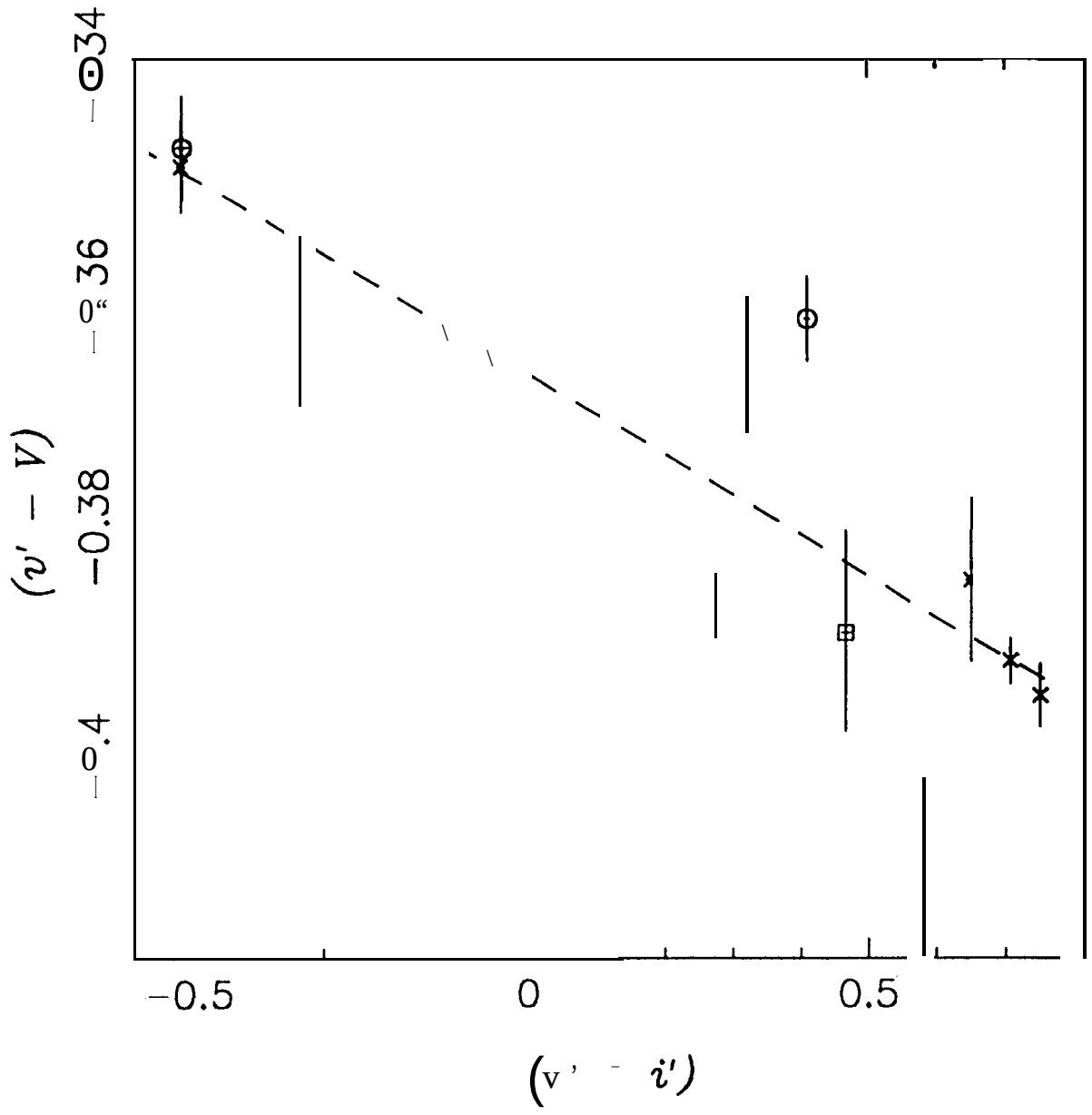

Fig 1d

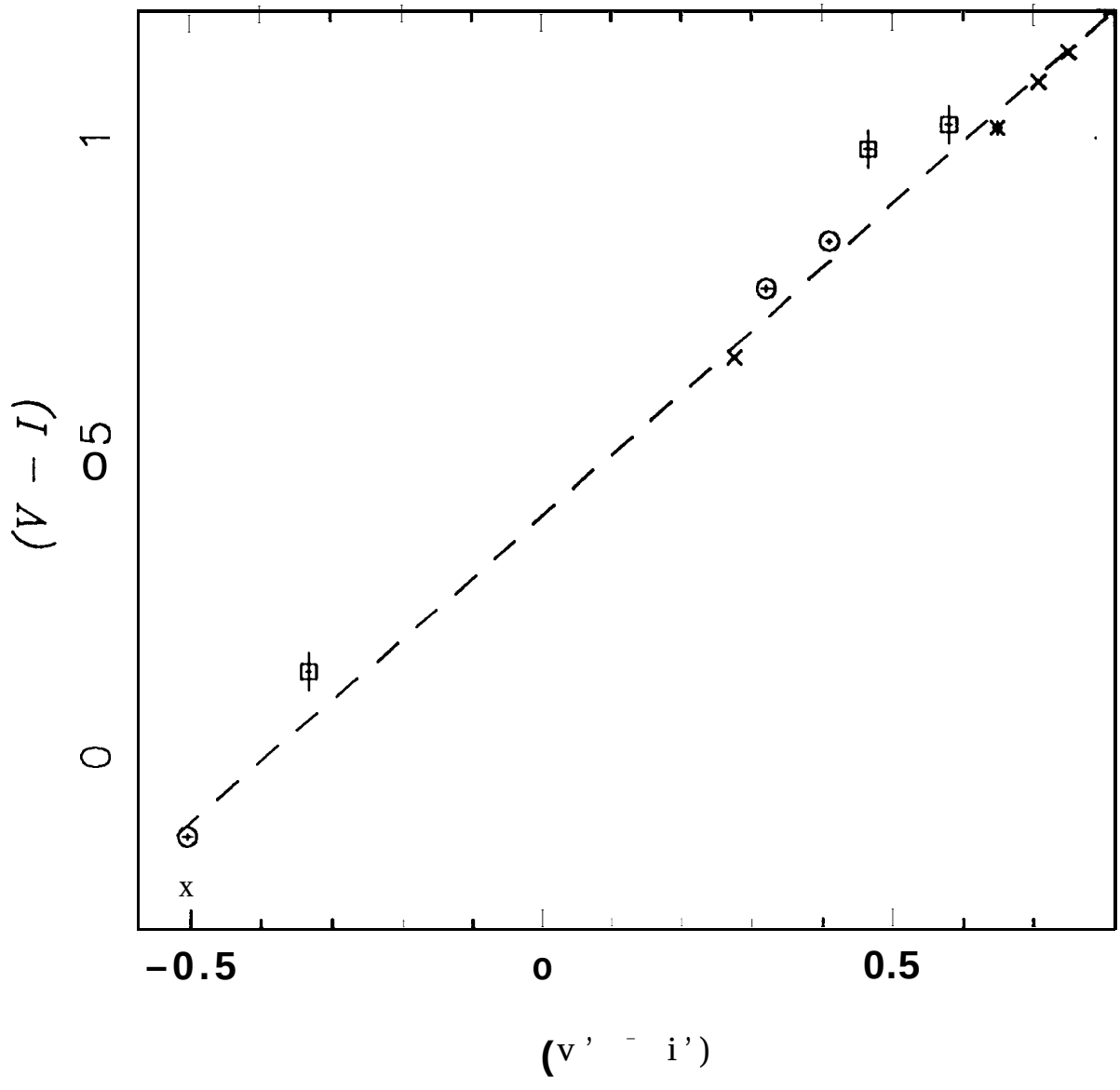

Fig 2

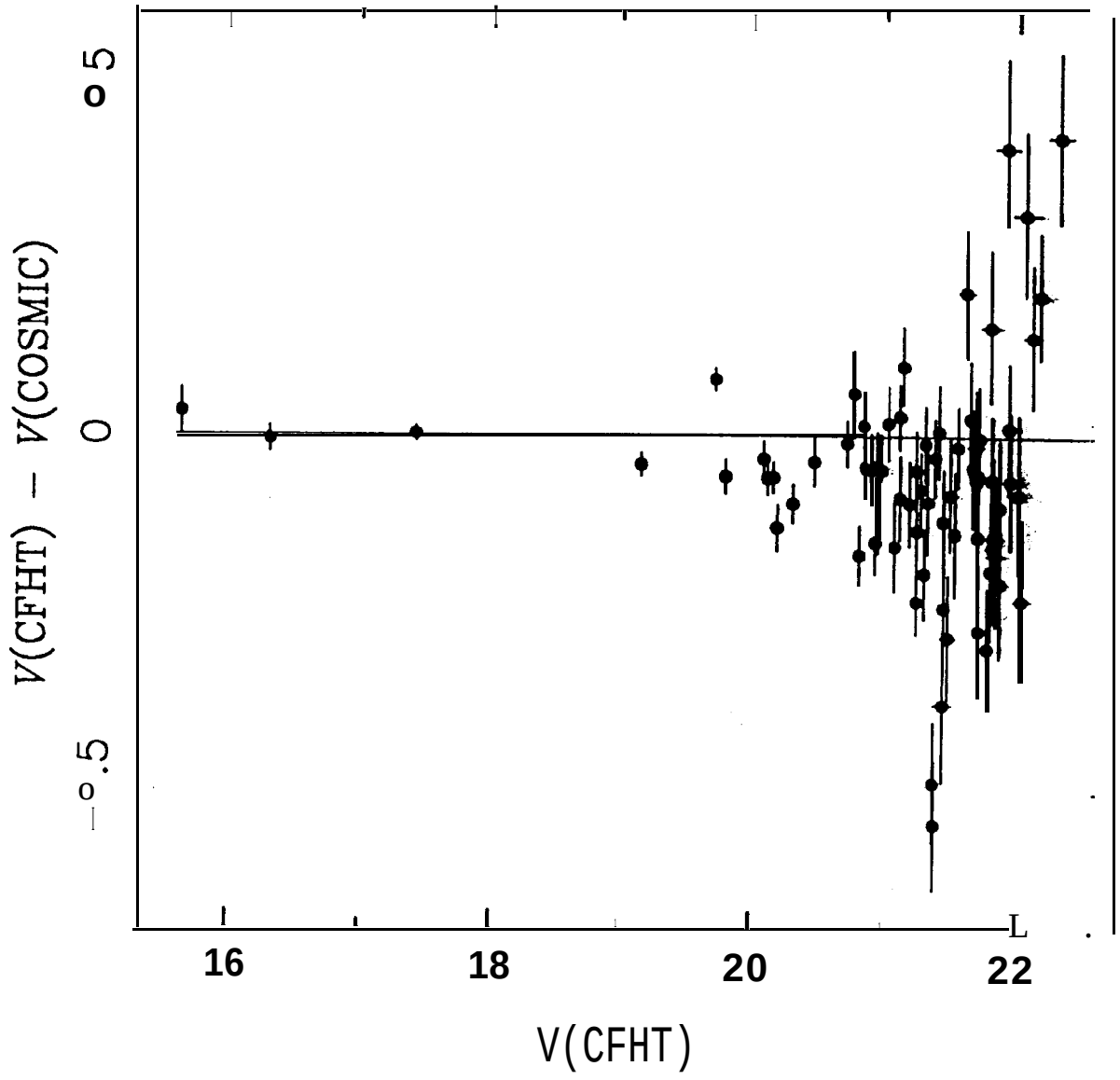

From order! match_plotter, using CFHT_V308

Fig 4

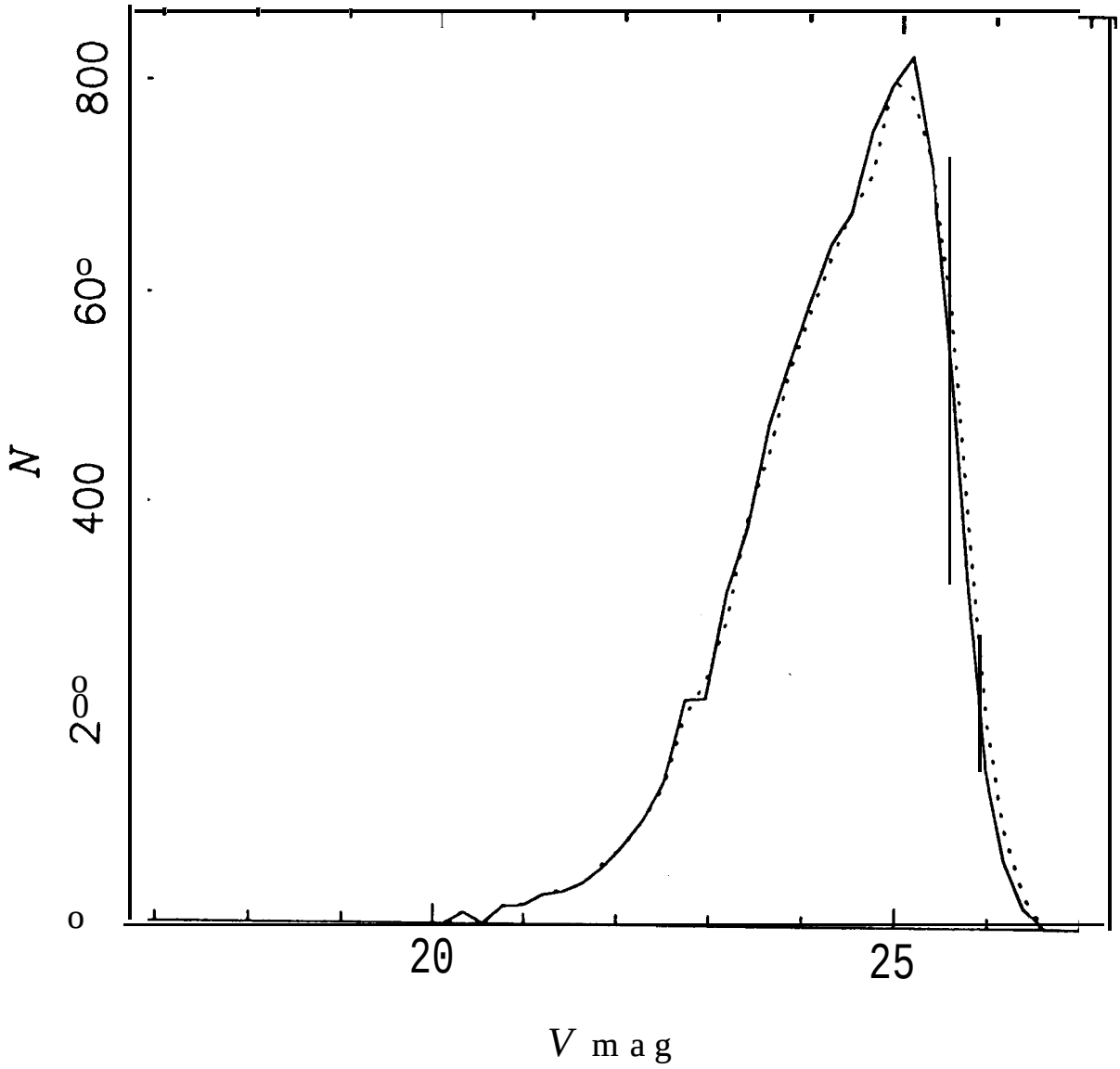

From /scr/smh/hst/m81/prog/cal-lumsig-plot

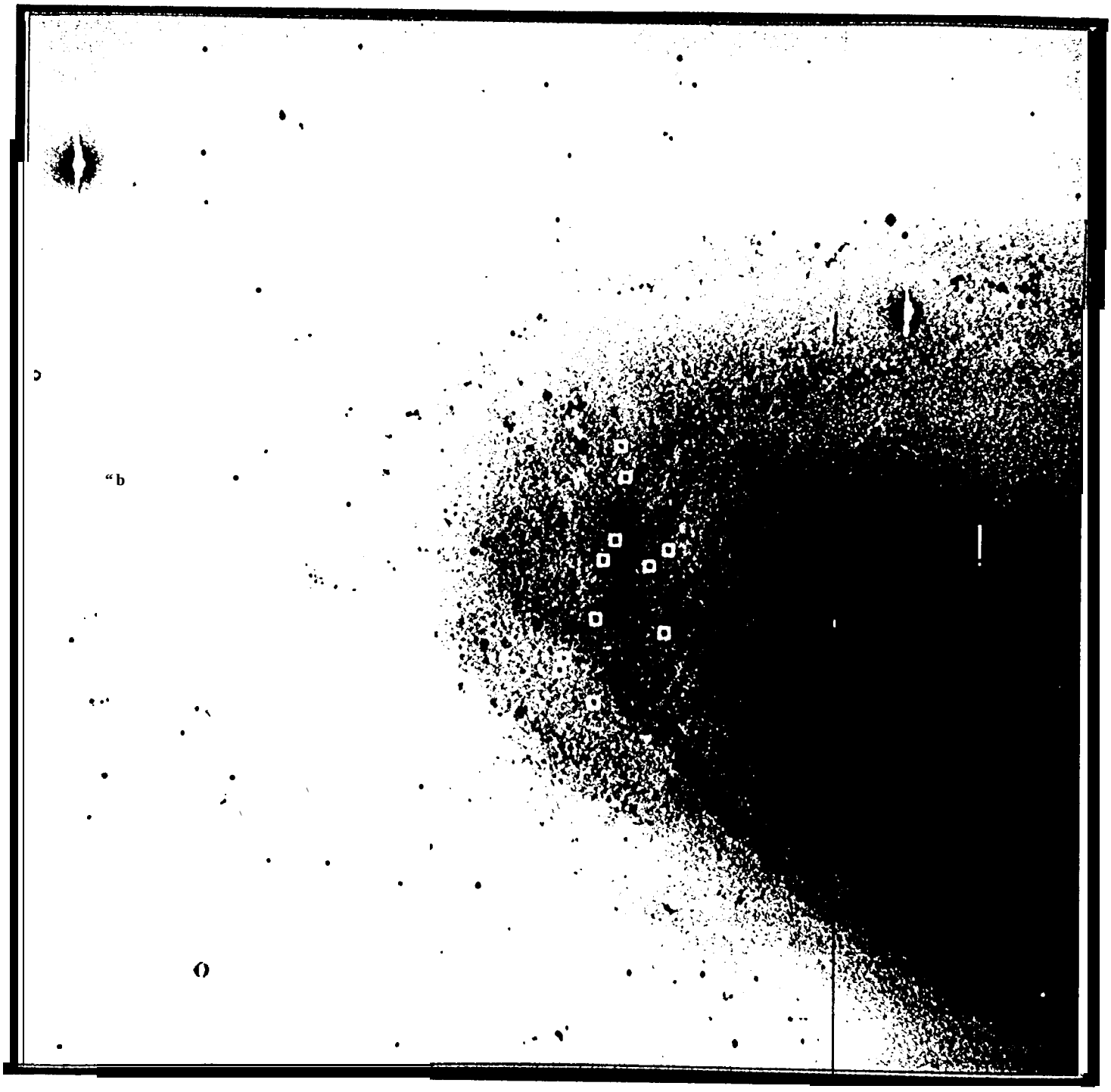

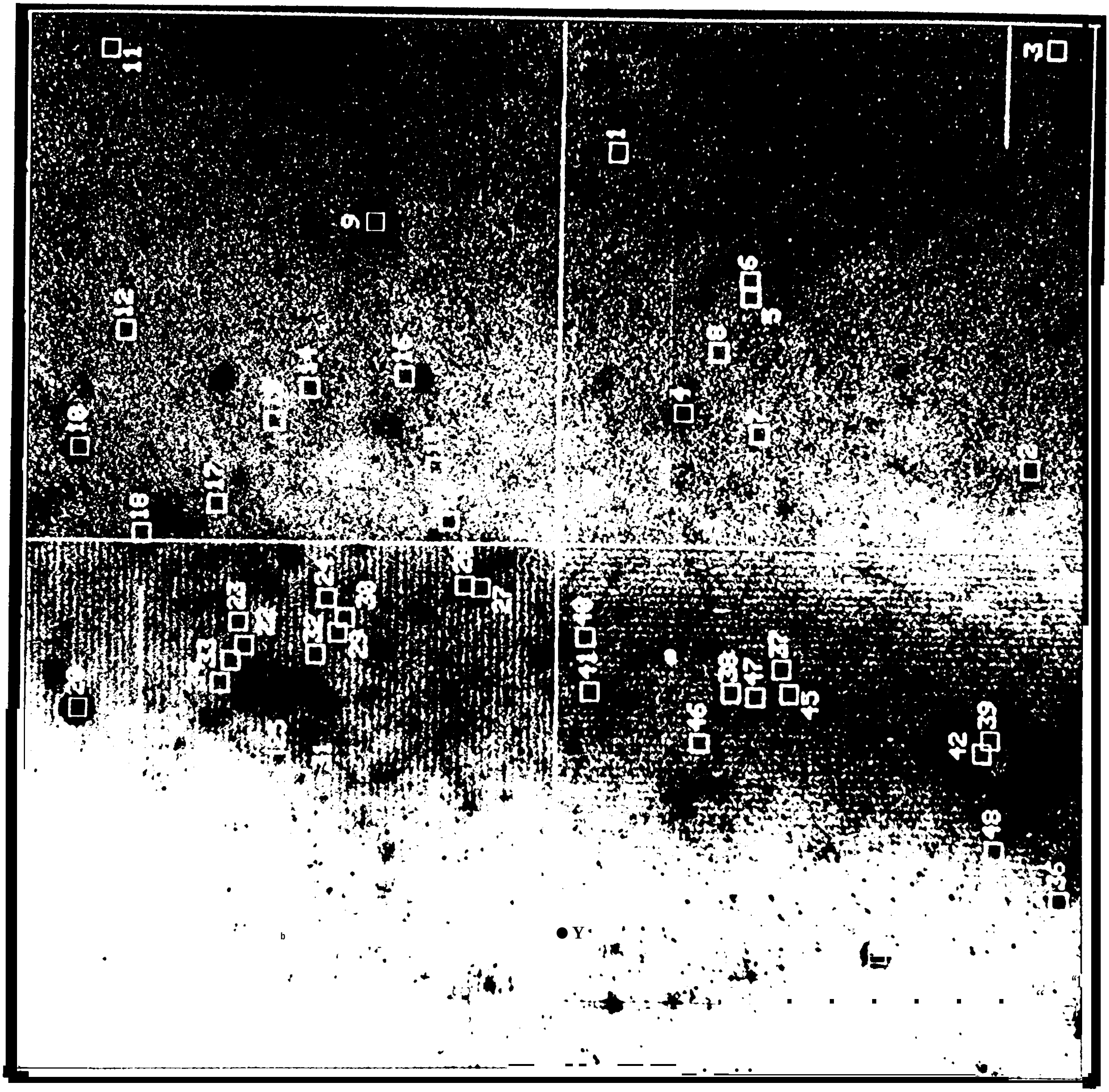

D16
D14
D9
D8

Fig 5